EDINBURGH INSTRUMENTS

50 YEARS 1971-2021

PRECISION RAMAN

Best-in-class Raman microscopes for research and analytical requirements backed with world-class customer support and service.

edinst.com

Received: 2 February 2021 | Revised: 10 June 2021 | Accepted: 30 June 2021

DOI: 10.1002/jrs.6203

SPECIAL ISSUE - RESEARCH ARTICLE

Journal of RAMAN SPECTROSCOPY WILEY

Raman studies on zoisite and tanzanite for gemmological applications

Alessia Coccato[1] | **Danilo Bersani**[2] | **Maria Cristina Caggiani**[1] | **Paolo Mazzoleni**[1] | **Germana Barone**[1]

[1]Department of Biological, Geological and Environmental Sciences, University of Catania, Catania, Italy

[2]Department of Mathematical, Physical and Computer Sciences, University of Parma, Parma, Italy

Correspondence
Alessia Coccato, Department of Biological, Geological and Environmental Sciences, University of Catania, Corso Italia, 57, 95127 Catania, Italy.
Email: alessia.coccato@unict.it

Funding information
"Programma ricerca di Ateneo UNICT 2020–22 linea 2" of the Department of Biological, Geological and Environmental Sciences, University of Catania

Abstract

Tanzanite is the blue to violet-blue variety of the sorosilicate zoisite; its colour is due to vanadium substitution of aluminium in the octahedral sites and is proved to appear after natural or artificial heating to approximately 500°C. Its colour makes it a highly appreciated gemstone, for this reason often imitated or thermally treated with the aim of enhancing its hue. Tanzanite loose gemstones are easily identified by classical gemmology methods that are not always applicable to mounted jewels. At the same time, zoisite Raman spectra are rarely reported in literature and never with a systematic approach. In this work, zoisite samples and cut tanzanite gemstones were considered, with the aim of filling this gap by addressing different methodological aspects. Namely, the orientational effects were investigated to explain the spectral variability, the photoluminescence bands were differentiated from the Raman signals using different excitation wavelengths, and the effectiveness of portable instrumentation in the correct identification of tanzanite was evaluated. The results are encouraging, showing that zoisite is revealed, notwithstanding orientational effects, by both portable and laboratory Raman instruments with comparable performances, opening the way to an effective identification of mounted tanzanite gemstones. Furthermore, the employ of different excitation wavelengths allowed to distinguish the photoluminescence bands with both categories of devices, thus identifying rare earth elements (REEs) likely associated with the mineral's genesis.

KEYWORDS

orientational effects, photoluminescence, portable Raman spectroscopy, tanzanite, zoisite

1 | INTRODUCTION

Tanzanite is the commercial name of the blue to violet-blue variety of zoisite mineral, a sorosilicate of ideal formula $Ca_2Al_3(Si_2O_7)(SiO_4)\cdot O(OH)$. Zoisite crystallizes in the dipyramidal class of the orthorhombic crystal system, in the *Pnma* space group.[1]

Mineralogically, it was recently distinguished from the epidote group, as it displays one single type of silicatic chains of SiO_4 tetrahedra sharing one oxygen, isolated

SiO_4 units, with two nonequivalent single chains of AlO_6 octahedra, and two irregular nonequivalent cavities occupied by calcium, either in sevenfold coordination[2–4] or nine to tenfold coordination.[5]

Zoisite is formed in low-to-medium grade metamorphic rocks and is found in numerous localities, including the Alps (Saualpe in Carinthia, Austria, where it occurs in eclogites[6]) and Corse.[7] So far, gem-quality tanzanite, the blue to violet-blue variety of zoisite, is only found in the Merelani area, Tanzania, which is part of the Neoproterozoic Mozambique Metamorphic Belt (NMMB), a very interesting geological setting for gem mineralization as the numerous faults associated with the N-S oriented rift create peculiar metamorphic conditions.[4,8,9] The formation of tanzanite is due to the infiltration of highly reducing, low viscosity hydrothermal solutions enriched in Ca, Mg, CO_2, SO_3, trace elements (Mn, Ti, V, Fe, U, Sr & Zn) and heavy rare earth elements (REEs) through graphitic gneisses, dolomitic marbles and schists.[2,4,9,10] It appears that tanzanite is formed through a garnet intermediate (tsavorite grossular) in quartz veins in anticlinal folds undergoing retrograde metamorphism.[8,9] It is often associated with other coloured zoisites (brown & yellow), green grossular garnet, diopside, quartz, graphite and calcite.[2] Common inclusions are graphite and sulphides; hence, the typical smell is released during cutting and polishing.[4]

From the gemmological point of view, its violet-blue colour makes the gem particularly appealing,[11,12] so that imitations are found in the market,[13] and treatments have been reported,[14] such as heating or coating.[2,3,14,15] The heating process is known to cause weaknesses that could provoke shattering of the crystal if inclusions are present; on the other hand, such inclusions could be even used to detect heating treatments.[15]

Moreover, natural dichroic tanzanites have been reported, but the uncertainties in the mining process do not allow for conclusive indications in this direction.[2,4] Nevertheless, it is reported that H_2S inclusions presence and dimensions can give an indication on the heating temperature of tanzanite up to 600°C.[15]

The colour of tanzanite is due to its vanadium content, deriving from organic graphite deposited within the gneiss host rock of tanzanite,[2,9] substituting for aluminium in the octahedral sites.[1,16,17] Moreover, tanzanite displays pleochroism, that is, shows different colours according to the observation direction: blue, purple and brown.[17] Most natural tanzanites are brownish and show trichroism, whereas the blue colour seems associated to heating to approximately 500°C, either natural,[2] that is associated to metamorphism[4] (ca. 10% of the market[17]), or artificial.[3] During this process, the mineral becomes dichroic,[17] with the 455-nm absorption band disappearing. This has been explained alternatively as increasing V^{4+} content,[18] or to changes in vanadium oxidation state: reduction to V^{3+}[17], or oxidation to V^{5+}[3]; pleochroism in tanzanite can be observed using a dichroscope.

Other ions have been reported for coloured zoisites and tanzanites,[2] but the relationship with colour is not always evident: pink zoisite (thulite) owes its colour to Mn^{3+} in M sites.[1] The ratios V/Ti and V/Cr seem also to have a significant role,[2,9] whereas strontium, substituting for calcium in the irregular A sites, seems somehow associated with colour.[2]

A distinctive content of neodymium has been reported in numerous minerals from the Merelani area, such as tremolite, diopside and grossular.[2,8] The trace element patterns reported in literature do not highlight any specific trend, suggesting that they can vary according to the immediate surroundings.[9]

Gem quality samples range from perfectly clear, violet-blue crystals that are cut to enhance transparency and colour, whereas the fractured ones, showing inclusions, are often polished into cabochons and rounded beads.[9] For samples showing cracks and inclusions, the heating treatment could result in permanent damage to the gem.[15]

Tanzanite can be easily identified from its refractive indices (RI, three pairs, one for each crystallographic axis) and specific gravity (SG), which are diagnostic among the blue and violet-blue gemstones. However, both approaches are inapplicable to investigate mounted gemstones.

Gems are intrinsically precious and their characterization poses numerous challenges. The identification of mineralogical species should be performed non-invasively, also considering that gemstones can be found in archaeological and historical artefacts. In the specific case of tanzanite, it has become commercially available since the 1960s.

X-rays fluorescence (XRF) analysis and Raman spectroscopy (RS), also available as portable instruments (pXRF and pRS, respectively), proved successful in the identification of gemstones used in different epochs.[13,19–28] XRF has started to be extensively applied to gemstones' trace elements study, even if less sensitive than other techniques especially to low Z elements, for its ease of use and nondestructiveness, in order to evaluate chromophores and provenance markers.[21,29–32]

Photoluminescence (PL) is a well-known phenomenon, often overwhelming the Raman effect. Its main gemmological application is in the field of diamond studies.[29,33] It is nevertheless an interesting tool to investigate trace elements such as neodymium, praseodymium and samarium in various minerals of geological and gemmological interest.[5,29,34–38] In the case of tanzanite, the features of vanadium ions have been tentatively

identified in photoluminescence spectra.[35,37–39] However, these features at 691 and 709 nm appear very similar to Cr^{3+} R-lines observed in minerals and gemstones.[38,39]

Tanzanites have rarely been studied by XRF and Raman spectroscopy in a gemmological context,[2,9,13] whereas literature is available about the geological meaning of this mineral.[8,40–42] Raman spectroscopic data on tanzanite are also rarely found. Whereas zoisite is reported in other studies,[35,43–45] micro-Raman studies of inclusions are also reported.[46–48]

In order to fill the existing gap in the literature, this paper aims at clarifying the following aspects concerning Raman spectroscopic characterization of gem-quality zoisite: (1) assess the orientational effects in zoisite samples, in order to explain spectral variability; (2) discriminate among photoluminescence bands and Raman signals thanks to the use of different excitation wavelengths; and (3) evaluate the effectiveness of portable instrumentation in correctly identifying tanzanite.

2 | MATERIALS AND METHODS

2.1 | Materials

Seven cut tanzanite gems (Figure 1), for which no information on the heating is available, were provided by a local jeweller. As a comparison, a zoisite from Tanzania, the only known provenance for gem quality tanzanite, was also studied (RZ): this sample shows the yellowish colour typical of many unheated tanzanites. In order to include a standard material, from a completely different location, a brownish zoisite sample from Passo del Gries, in the Lepontine Alps between Italy and Switzerland was considered for comparison (AZ, Figure 1). All the samples belong to private collections. Table 1 summarizes their macroscopic features, including shape and cut, colour, features, size and weight.

2.2 | Methods

Optical properties of the cut gemstones were obtained with a polariscope and a duplex refractometer, using a contact liquid with refractive index (RI) = 1.79. The refractive indices were only measured on the table of the faceted gems. SG values were obtained, when possible, by dividing the weight in air by the difference between the weight in air and in water, the latter measured with a hydrostatic balance.

Three gems were measured with a portable Bruker Tracer IV-SD XRF system equipped with an Rh-target X-ray tube, Pd slits and a Silicon Drift Detector. Two spectra of 60 s (livetime) were collected on each gem (15 kV and 35 μA for major elements & 40 kV and 17 μA for traces). Quantitative data were obtained by fundamental parameter method using PyMCA software,[49] with configuration files adapted for the Tracer IV-SD specification and considering zoisite as matrix. Major and trace elements data were corrected using the best fit method (42 international minerals and rocks standards).

Raman measurements were carried out with different instrumentations (Table S1), both fixed and mobile, provided with different excitation wavelengths, displaying different spectral ranges, spatial and spectral resolutions.

In the case of AZ sample, moreover, spectra were collected considering the crystallographic axes following the observation of the crystal habit.

2.2.1 | Laboratory devices

In order to ensure the correct calibration of the laboratory instruments, the position of the main Raman band of Si at 520.7 cm^{-1} was checked.

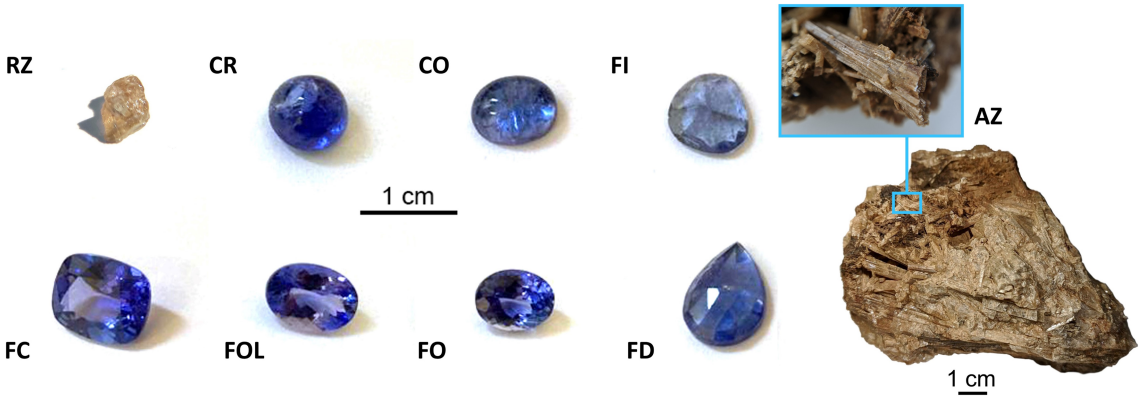

FIGURE 1 Photographs of the analysed samples and detail of the AZ crystals used for polarized Raman measurements

TABLE 1 Overview of studied samples and performed analyses

Code	Cut	Shape	Colour	Features	Dimensions (mm)			Weight (ct)	Classical gemmology	Micro-RS (nm) 473, 532, 633, 785	Portable RS (nm) 532, 785	PXRF
AZ	Massive sample		Brownish	Macroscopic sample	—			—	No	473, 633	532	No
RZ	Rough sample		Yellowish		Maximum dimension ca. 6			—	No	473	532	No
CO	Cabochon	Oval	Blue	Fractured, dark inclusions	10.20	8.20	4.50	3.70	SG only	532, 785	785	Yes
CR	Cabochon	Round	Blue	Fractured	9.10		7.75	4.85	SG only	532, 785	785	Yes
FI	Faceted	Irregular	Pale blue	Fractured	10.05	9.60	1.85	1.82	Yes	532, 785	785	No
FOL	Faceted	Oval	Blue, indigo	Transparent	11.00	8.10	5.15	3.35	Yes	532, 785	785	Yes
FO	Faceted	Oval	Blue	Transparent	9.35	7.45	5.30	2.70	Yes	532, 785	785	No
FD	Faceted	Drop	Blue	Transparent, fractured	13.60	9.75	3.70	4.22	Yes	532, 785	785	No
FC	Faceted	Cushion	Deep blue	Transparent	12.10	9.95	5.95	5.40	Yes	532, 785	785	No

Abbreviation: SG, specific gravity.

- A Jasco NRS 3100 microspectrometer equipped with 785- and 532-nm lasers, focused on the samples through a 50× long working distance objective with a spot size approximately 2 μm. A 600 grooves per millimetre grating was used, together with a confocal slit of 0.5 × 6 mm. The green laser was operated at approximately 4 and 8 mW, and the near-infrared (NIR) one at approximately 25 and 50 mW on the sample, for the low wavenumber (up to 1200 cm^{-1}) and OH regions, respectively. With each laser, at least three measurements were acquired on each sample, consisting of 20 accumulations of 30 s.
- A Horiba LabRam micro-Raman equipped with blue and red excitations was used. A 20-mW 633-nm laser, and a 100-mW, 473-nm one were used in combination with a 1800 grooves per millimetre grating. A 50× long working distance objective was used to focus the laser, delivering approximately 1 mW on the sample. Two accumulations of 30 s were acquired for each point.
- A Horiba LabRam Evolution HR micro-Raman. The configuration used for measurements in controlled polarization includes a 632.8-nm He-Ne laser, a 1800 grooves per millimetre holographic grating, Bragg filters for very low-wavenumber rejection of the Rayleigh line, a 50× ULWD objective, a polarizing analyser. Laser power was kept below 1 mW on the sample. The CCD detector is cooled with liquid nitrogen. The spectral resolution was nearly 0.5 cm^{-1}.

2.2.2 | Portable devices

- An i-Raman BWTek spectrometer was used. The 785-nm diode laser source, operated at 60 mW, was focused on the sample through a 1.5-m fibre-optic probe working in contact with a spot size approximately 0.5 mm. A holographic grating disperses the backscattered light on a Peltier-cooled CCD detector (−4°C). Three repetitions of 10 s were acquired on the table and on the pavilion of each sample, covering the whole range up to approximately 3300 cm^{-1}.
- An EnSpectr-handheld RaPort spectrometer was employed for the characterization of the RZ sample. The instrument is equipped with a 30-mW, adjustable power, 532-nm laser and a thermoelectrically cooled detector, which allows to investigate the spectrum up to approximately 4000 cm^{-1}. The spot size is of approximately 0.5 mm.[50] The total measurement time for this study was of 120 s.

All the used lasers are linearly polarized and, in absence of polarizing analysers, all the used instruments have a preferential input direction, in a variable amount, parallel to the laser polarization. So the majority of spectra should be considered having prevalent 'xx' polarization where the x is the polarization direction of the laser. Photoluminescence was observed in the Raman spectra and vice versa.

3 | RESULTS

3.1 | Classical gemmology, pXRF

The classical gemmology results all agree on the gems being tanzanite, the blue to violet-blue coloured variety of the sorosilicate zoisite.

Table 2 summarizes the results of classical gemmology analyses. Reported SG and RIs, measured on the faceted gemstones only, are consistent with tanzanite.[4]

From pXRF analyses conducted on samples FOL, CO, CR (Table 3), representative of different hues and colour

TABLE 2 Results of classical gemmology characterization of the gem quality samples

Sample	SG	RI1	RI2	Birefringence
CO	3.25	Not determined		
CR	3.34			
FI	3.31	1.696	1.704	0.008
FOL	3.42	1.692	1.708	0.016
FO	3.51	1.698	1.702	0.004
FD	3.30	1.692	1.700	0.008
FC	3.40	1.689	1.694	0.005

TABLE 3 Quantification results of pXRF chemical analyses of selected tanzanite samples

	CO	FOL	CR
Al_2O_3	25.86	27.06	26.26
SiO_2	44.89	44.19	44.91
CaO	29.26	28.75	28.83
Ti	7.02	6.94	7.27
V	8.74	7.28	12.18
Cr	1.03	0.87	1.39
Mn	0.51	0.76	0.76
Fe	5.83	6.03	6.34
Sr	87.05	260.90	101.60
V/Ti	1.24	1.05	1.68
V/Cr	8.47	8.41	8.78

Note: Values are reported as wt% for the oxides (Al_2O_3, SiO_2, & CaO), whereas trace elements are in ppm. Data were corrected considering the measurement settings and a zoisite matrix in PyMCA.

TABLE 4 Summary of Raman band positions representatively shown by zoisite and tanzanite samples in this work

	This study										
	473	473	532	532	532	633 AZ					785
	AZ	RZ	AZ	RZ	FI						FOL
Mode						$z(xx)\bar{z}$	$z(yy)\bar{z}$	$y(zz)\bar{y}$	$z(xy)\bar{z}$	$y(xz)\bar{y}$	$x(yz)\bar{x}$	
B_{3g}											65	
A_g						84						88
B_{2g}										102		104
$A_g + B_{1g}$						118	119	120	119			122
B_{2g}										129		
A_g	153	152	148	150	151	147	149	148				150
B_{2g}										160		
A_g	194	192	189	190	190	191	192	192				192
B_{1g}			213						214			217
B_{2g}										227		232
A_g	263		262	261	262	259	259	260				263
B_{2g}		267								264		
B_{1g}									279			
A_g			281			284	285	283				280
B_{3g}	289	291	288	288	289						287	288
B_{3g}			311	312	312						308	
A_g	316	316				313	313	313				313
B_{2g}										328		
A_g			337			336						338
A_g			345	343	344		345	346				346
B_{3g}	349										348	
B_{1g}			394						394			
B_{3g}				400							397	397
A_g	423	422	419	416	419	419	419	420				419
B_{2g}										432		435
A_g	441	436	436	436	440			437				
$A_g + B_{2g}$	459	459	455	456		456		456		455		457
A_g					477		476					478
B_{1g}									486			
A_g (+B_{2g}?)	495	496	490	492	492	491	491	492		492		494
B_{3g}											514	
A_g	531	532	528	528	524	527	527	528				528
A_g		542				537						537
B_{1g}									550			
A_g	575	579	571	573	573	572	572	570				575
A_g	601	599	596	597	596	595	596	596				598
B_{1g}			622						618			623
A_g	626	625			625	625	624					
B_{3g}			649								653	
B_{1g}									659			

(Continues)

TABLE 4 (Continued)

	This study											
	473	473	532	532	532	633 AZ						785
Mode	AZ	RZ	AZ	RZ	FI	$z(xx)\bar{z}$	$z(yy)\bar{z}$	$y(zz)\bar{y}$	$z(xy)\bar{z}$	$y(xz)\bar{y}$	$x(yz)\bar{x}$	FOL
A_g	682	681	674	677	677	677	677	677				679
A_g			688	694			692	695				691
A_g			734			726		726				
A_g			776		775	773	777					783
B_{2g}										834		
A_g			842			845						839
$B_{3g} + B_{1g}$									860		861	
A_g	875	876	870	873	870	873	872	871				874
A_g	895	896	887			887	890	887				888
B_{3g}											901	
B_{1g}									910			912
A_g	931	932	926	927	927	928	927	926				928
B_{1g}									947			
A_g	989	986	982	984	981	983	983	983				984
A_g	1075	1076	1070	1072	1070	1072	1071	1072				1073
A_g	1092	1097	1089	1092	1091	1092	1091	1092				1093
A_g					3153			3163		3163		
A_g								3249				

Note: The laser wavelength in nm is indicated in the second row. Values are in cm^{-1}.

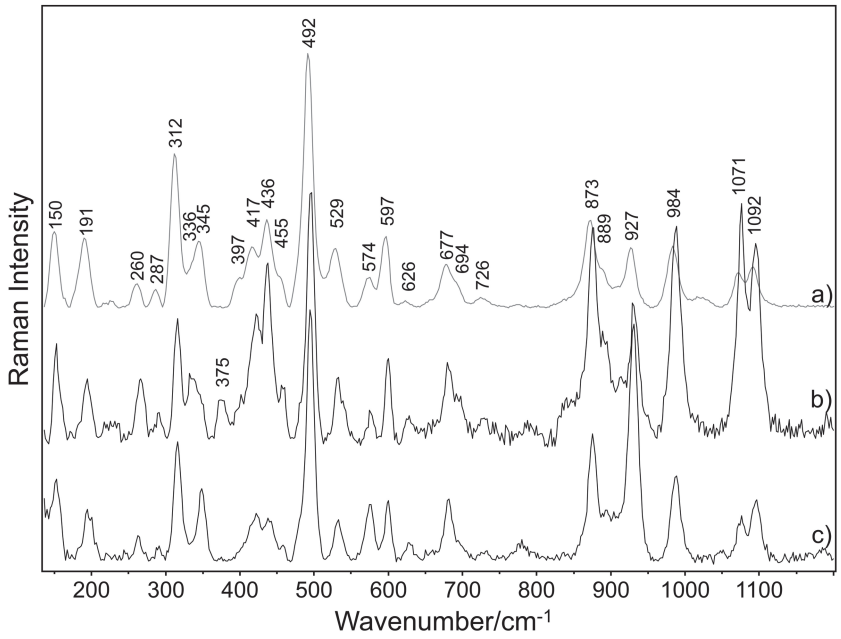

FIGURE 2 Raman spectra of Tanzania rough sample (RZ, spectra a and b) and Alpine zoisite (AZ, spectrum c) obtained with 532- (grey line, spectrum a) and 473-nm (black lines, spectra b and c) lasers. Spectra are baseline corrected, normalized to the band at 492 cm^{-1}, and stacked for clarity

saturation, the weight % average values for SiO_2, Al_2O_3 and CaO are in good agreement with what reported in literature.[9] V, Ti and Cr are proportionally higher in sample CR, whereas Sr content is highly variable among the studied samples.

3.2 | Raman spectroscopy

The representative Raman band positions, in accordance with literature data (Table S2), of zoisite (AZ) and tanzanite (RZ; FI and FOL gems) analysed in this study are reported in Table 4. To the authors' knowledge, it is the first time that the Raman spectrum of zoisite is reported with a 473-nm excitation. Moreover, the low wavenumber (65, 88 and 105 cm^{-1}) bands of tanzanite are observed (Table 4).

The Raman spectra of AZ and RZ samples acquired with 532- and 473-nm lasers are displayed in Figure 2: the bands show different relative intensities depending on the measured point. Figure 3 shows spectra acquired on different points of a cut gemstone with the 532-nm laser, highlighting a similar behaviour to zoisite spectra (Figure 2). Variability in the spectra affects both the low and high-wavenumber region of the Raman spectrum[35]: as the OH region was also investigated, the two bands at approximately 3150 and 3535 cm^{-1} are also shown to be orientation dependent, the former grouping together with those at approximately 340 and 925 cm^{-1}.

With the aim of better investigating the orientational effects, Raman spectra were acquired on AZ sample paying attention to the laser polarization, the scattering geometry and crystallographic axes.

3.2.1 | Orientational effects

Spectra acquired on AZ sample in different directions and with different polarizations using the 633-nm laser of the Horiba Labram Evolution HR fixed spectrometer are displayed in Figure 4. The scattering geometries are indicated using the Porto notation. Using the Bilbao Crystallographic Server[51] and a suitable crystallographic file,[52] we obtained the mechanical representation of zoisite (space group *Pnma*): 40 A_g + 26 A_u + 26 B_{1g} + 40 B_{1u} + 40 B_{2g} + 26 B_{2u} + 26 B_{3g} + 40 B_{3u}. The only Raman active modes are A_g (visible in parallel xx, yy and zz polarizations), B_{1g} (visible in xy polarization), B_{2g} (xz polarization) and B_{3g} (yz polarization). More than 60 vibration frequencies were found and are reported in detail in Table 4: 32 A_g (plus the OH vibrations), 11 B_{1g}, 9 (or 10) B_{2g}, 9 B_{3g}. Some of the weaker peaks present in the spectra relative to crossed polarizations seem to be the result of leakage of the parallel polarization: in that case, they are not accounted as different modes. On the other hand, the high intensity of the principal band at approximately 492 cm^{-1} may lead to hypothesize an additional B_{2g} component, apart the A_g one, for this signal (Table 4). OH stretching

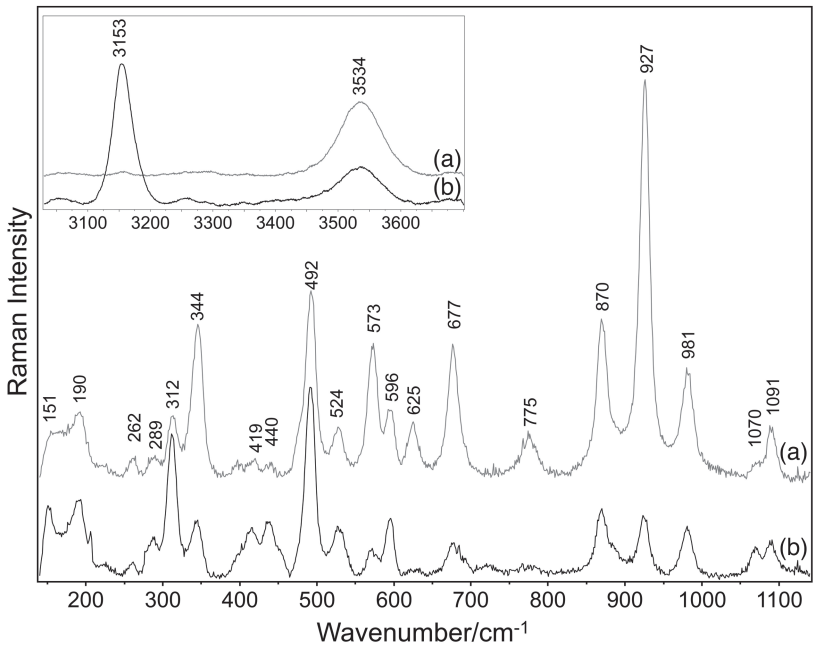

FIGURE 3 Raman spectra on different facets (a, b) of gem quality cut tanzanite (FI) with 532-nm laser. Spectra are baseline corrected, normalized to the band at 492 cm^{-1} and stacked for clarity. The inset shows the high wavenumber region for both spectra

vibrations, probably referred to A_g modes, are only visible polarizing along the Z direction.

3.2.2 | Portable instrumentation effectiveness

Orientational effects are clearly visible also when portable instrumentation is used on loose gemstones, due to the linear polarization of the lasers equipping the devices.

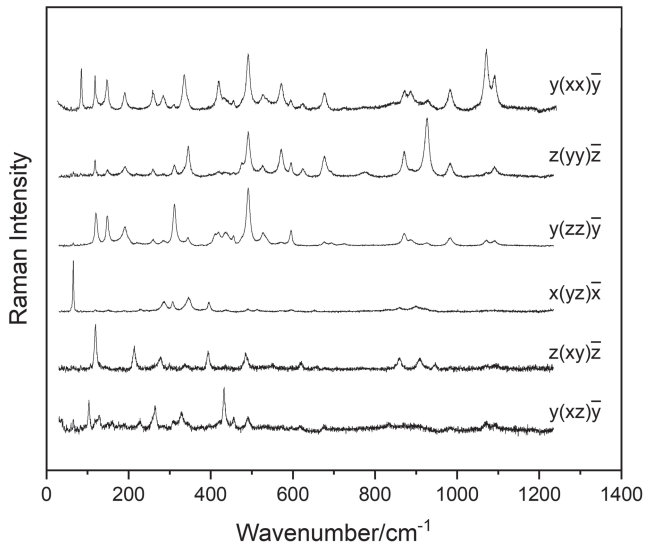

FIGURE 4 Raman spectra acquired on the different faces of the AZ crystal considering the crystallographic axes orientation. Porto notation is used to define the scattering geometry. Spectra are stacked for clarity

Figure 5 shows spectra acquired with the 785-nm laser on the table (a) and on the pavilion (b). These spectra clearly show the intrinsic variability of Raman spectra acquired on cut gemstones.

Moreover, as the 785-nm laser is used in this instrument, photoluminescence features of trivalent REEs are clearly visible. In Figure 5, the band at 1148 cm^{-1} actually corresponds to 863 nm, which is attributed to Nd^{3+}.[5,37] Photoluminescence is explored in more detail in the following paragraph.

3.2.3 | Photoluminescence

In Raman spectra acquired with 473-, 532- and 785-nm excitations, in addition to the expected Raman signals, extra bands can be seen (Table 5, Figures 5, 6 and 7). Band positions in nanometres are reported in Table 5. The 473-nm excited spectra of AZ and RZ samples are compared in Figure 6: photoluminescence bands are clearly visible in both samples, with RZ having stronger signals. The same is true for the spectra excited with the 532-nm laser. The band at 3150 cm^{-1} remains notwithstanding the used laser and is therefore a Raman band (Table 4).

On the other hand, the spectra reported in Figure 7, excited with the same laser and collected either with a portable or laboratory instrument, clearly show the same photoluminescence pattern, as expected.

Overall, the luminescence is attributed to trivalent REEs,[5,36,37] with RZ and cut gemstones (all from Tanzania) showing higher intensities than AZ (from the Alps), which is consistent with tanzanite's genesis.

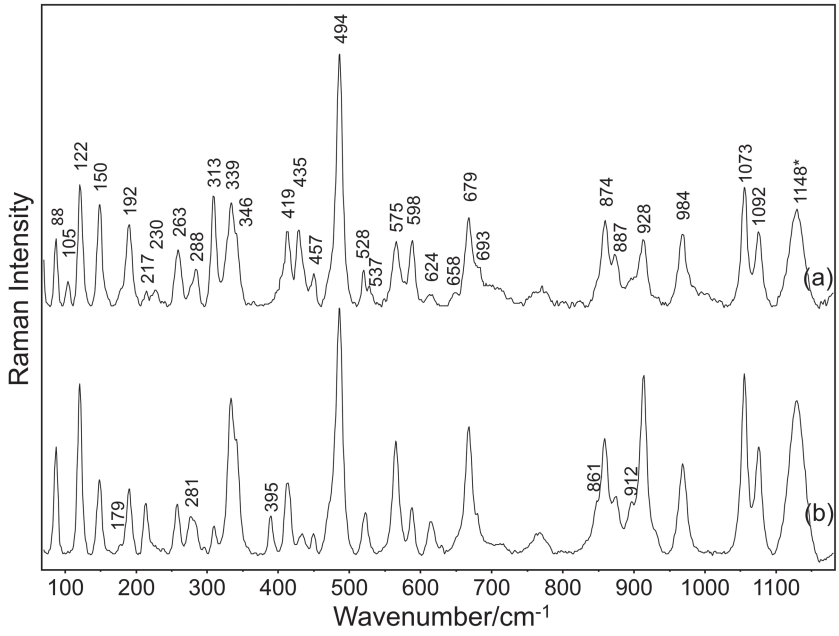

FIGURE 5 Portable Raman spectra of gem quality cut tanzanite (FOL) with 785-nm laser: table (a) and pavilion (b). Spectra are baseline corrected, normalized to the band at 494 cm^{-1} and stacked for clarity. Labels marked with * indicate photoluminescence signals

TABLE 5 Observed photoluminescence bands and attribution according to literature

473 nm	Zoisite,[5] tanzanite[36]	532 nm	Zoisite,[5] tanzanite[37]	785 nm	Zoisite,[5] tanzanite[37]
481	Dy^{3+}	556	Nd^{3+}	863	Nd^{3+}
598	Sm^{3+}, Eu^{3+}	573	Sm^{3+}, Dy^{3+}, Eu^{3+}	872	Nd^{3+}
602	Eu^{3+}	579	Sm^{3+}, Dy^{3+}, Eu^{3+}	880	Nd^{3+}
604		586	Sm^{3+}, Eu^{3+}; REE	890	Nd^{3+}
		588	Dy^{3+}, Nd^{3+}, Eu^{3+}; REE	896	Nd^{3+}
		590	Sm^{3+}, Eu^{3+}	899	Nd^{3+}
		596	Sm^{3+}, Nd^{3+}, Dy^{3+}, Nd^{3+}, Eu^{3+}	910	Nd^{3+}
		611	Sm^{3+}, Eu^{3+}	913	
		617	Sm^{3+}, Cr^{3+}, Eu^{3+}	1052	Er^{3+}, Nd^{3+}
		621	Sm^{3+}, Cr^{3+}, Eu^{3+}	1062	Nd^{3+}
		623	Sm^{3+}, Cr^{3+}, Eu^{3+}	1066	Nd^{3+}
		655	V^{2+}, Cr^{3+}[35]	1069	Nd^{3+}
				1083	Er^{3+}

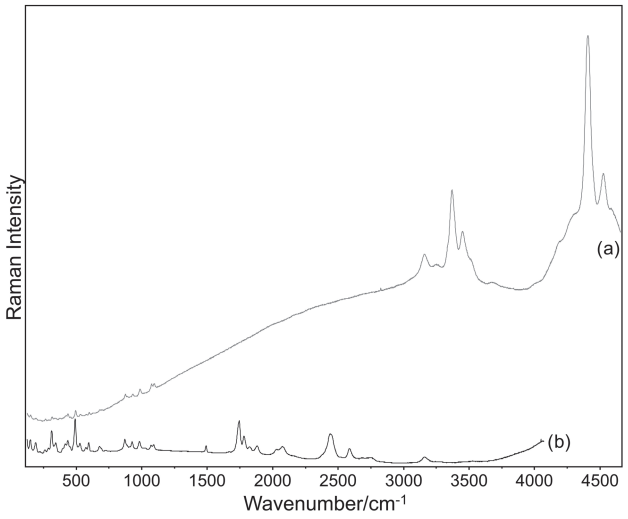

FIGURE 6 (a) 473- and (b) 532-nm excited Raman and photoluminescence spectra of Tanzania rough sample (RZ)

4 | DISCUSSION

Even though in general the Raman band positions are the same with all lasers, a few interesting aspects should be highlighted from Table 4. The spectra acquired with different lasers allowed to verify that a general good agreement exists in band positions. However, different peak shape and relative intensities are dependent on the spectral answer of detectors in each wavelength range. Moreover, as the observed Raman band positions' shifts are not systematic across the different spectra (Table 4), it does not appear that this aspect can be simply explained by different instrumental calibrations. These shifts can be due to compositional variations or to unresolved doublets causing apparent shifts.

The effect of the different orientation of zoisite crystal is clearly visible looking at the significant changes in relative intensities of the peaks. The results obtained are in agreement with the oriented (0.0 and 90.0°ccw) RRUFF spectra of zoisite even though not all the cases are there reported.[53] The spectra seem in accordance with those shown by Weis et al[35] too, where on the other hand, the parallel and crossed polarization contributions are not separated and the signals are not exhaustively listed. Few bands, the more intense ones of the parallel polarization spectra (at about 120, 490, 1070 and 1090 cm^{-1}), are almost constantly present, even though with highly variable intensity. In the crossed polarization spectra, the bands at approximately 65, 120 and 430 cm^{-1} are the principal signals, respectively, referable to B_{3g}, B_{1g} and B_{2g} modes. Consequently, it appears evident that reporting all the possible and complete signatures constitutes an essential reference to ensure zoisite identification when only the most intense bands are visible and/or when orientation cannot be recognized in the sample to be analysed (Table 4). The spectra obtained on zoisite with the 633-nm laser (Table 4, Figure 4), indeed, can be useful as reference to evaluate an uncertain orientation. As an example, variability is also observed in the spectra of tanzanite cut gemstones obtained in this work without certain knowledge about the relationship between facets and crystallographic axes. Following the above mentioned data (Table 4, Figure 4), therefore, the spectrum (a) in Figure 3 could be associated to $z(yy)\bar{z}$ polarization, due to the high intensity of the 344- and 927-cm^{-1} bands

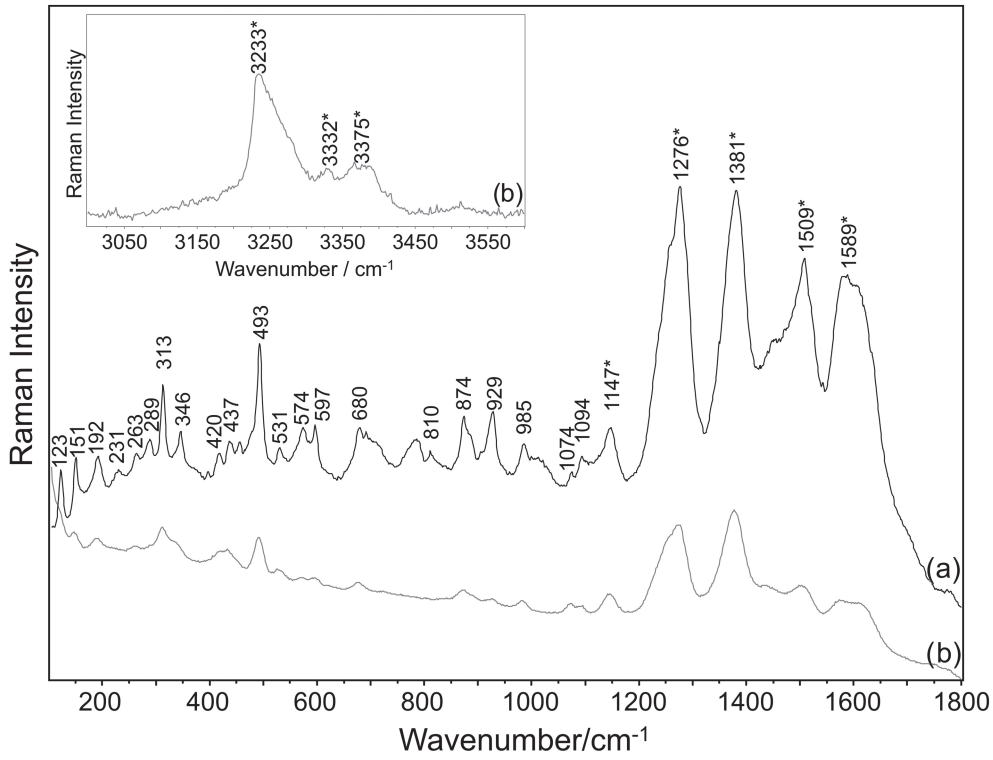

FIGURE 7 Raman and photoluminescence spectra of cut gemstone sample CR with 785 nm excitation, with a portable instrument (a) and fixed one (b). Labels marked with * indicate photoluminescence signals. The inset shows additional photoluminescence bands in the higher wavenumber region of spectrum (b). Spectra are stacked for clarity

and the very weak 3153 cm^{-1} one. On the other hand, the higher intensity of 312 cm^{-1} and the much lower one of 927 cm^{-1} peaks, together with the appearance of the strong OH-connected band (3153 cm^{-1}) lead to attribute spectrum (b) of Figure 3 to the $y(zz)\bar{y}$ polarization.

In terms of identification, portable Raman equipments give results comparable with the laboratory ones, providing good quality spectra in less than 60 s. The availability of different lasers is not required for the confirmation of tanzanite, because there is not a strong fluorescence background. Some spectrometers, allowing the recording of spectra in the region 1200–4000 cm^{-1}, offer the interesting possibility to study the OH vibrations (with blue or green excitation), and the wavelength-dependent photoluminescence.

As Raman spectra were collected with different laser sources, different luminescence centres could be excited (Table 5), such as Nd^{3+} and other trivalent REEs, as well as Cr^{3+}[5] consistent with tanzanite's genesis. Exciting with the NIR laser at 785 nm (Figure 5), it appears that all the bands above 1140 cm^{-1} are actually due to luminescence (Table 5) attributed to Nd^{3+}.[5,37]

5 | CONCLUSIONS

Although the identification of tanzanite, the blue to violet-blue variety of zoisite from the Merelani mines in Tanzania, can be successfully performed on loose gemstones by classical gemmology approaches, RS becomes necessary for the fast, univocal and contactless identification of mounted gemstones and for the investigation of museum objects and private collections.

The number of analysed samples and the range of Raman instruments and excitation sources used in this study allow an extensive characterization of zoisite and of tanzanite, leading to the definition of the range of variability for each peak of such a complex spectrum, further complicated by orientational effects and photoluminescence. In this way, the identification of the phase is made possible regardless the instrument employed, by taking into account the here observed variability. Outside this range, doubts concerning anomalous compositions or aggressive enhancement treatments should be considered. On the other hand, no clear differences in the Raman spectra could be highlighted between the zoisite samples from the Alps or from Merelani.

Both portable and laboratory instruments proved successful in identifying REEs likely associated with the minerals' genesis and present below the detection limits of pXRF, such as Nd^{3+}, Sm^{3+} and Eu^{3+}. These could allow to gain knowledge on the provenance and genesis of zoisite, considering the wavelength-specific response of REEs.

ACKNOWLEDGEMENTS

Dr U. Longobardo is acknowledged for providing the cut samples used in this study.

FUNDING INFORMATION

This work is supported by funds of the "Programma ricerca di Ateneo UNICT 2020–22 linea 2" of the Department of Biological, Geological and Environmental Sciences, University of Catania.

DATA AVAILABILITY STATEMENT

Data sharing not applicable to this article as no datasets were generated or analysed during the current study

ORCID

Alessia Coccato https://orcid.org/0000-0002-6641-2820
Danilo Bersani https://orcid.org/0000-0002-8026-983X
Maria Cristina Caggiani https://orcid.org/0000-0001-8475-1175
Paolo Mazzoleni https://orcid.org/0000-0002-9777-7857
Germana Barone https://orcid.org/0000-0003-0822-2436

REFERENCES

[1] G. Franz, A. Liebscher, *Rev. Mineral. Geochem.* **2004**, *56*, 1.
[2] R. Bocchio, I. Adamo, V. Bordoni, F. Caucia, V. Diella, *Period. di Mineral.* **2012**, *81*, 379.
[3] T. Pluthametwisute, B. Wanthanachaisaeng, C. Saiyasombat, C. Sutthirat, *Molecules* **2020**, *25*, 1.
[4] V. Zancanella, *Tanzanite. All about one of the most fascinating gemstones*, Naturalis Historia, Cavalese, Italy **2004**.
[5] M. Gaft, R. Reisfeld, G. Panczer, Rare-Earth Elements Luminescence in Minerals, **2015**.
[6] A. Mottana, W. R. Church, A. D. Edgar, *Contrib. To Mineral. Petrol.* **1968**, *18*, 338.
[7] M. Fournier, L. Jolivet, B. Goff, R. Dubois, *Tectonics* **1991**, *10*, 1173.
[8] J. Feneyrol, G. Giuliani, D. Demaiffe, D. Ohnenstetter, A. E. Fallick, J. Dubessy, J. E. Martelat, A. F. M. Rakotondrazafy, E. Omito, D. Ichang'I, C. Nyamai, A. W. Wamunyu, *Can. Mineral.* **2017**, *55*, 763.
[9] C. Harris, W. Hlongwane, N. Gule, R. Scheepers, *South African J. Geol.* **2014**, *117*, 15.
[10] B. Olivier, *The Geology and Petrology of the Merelani Tanzanite Deposits*, Stellenbosch University, NE Tanzania **2006**.
[11] B. Cairncross, *Rocks Miner.* **2019**, *94*, 530.
[12] B. Cairncross, *Rocks Miner.* **2020**, *95*, 458.
[13] L. Kiefert, S. T. Schmidt, *Gems Gemol.* **1996**, 270.
[14] S. F. McClure, A. H. Shen, *Gems Gemol.* **2008**, *44*, 142.
[15] A. H. Rankin, D. Taylor, P. J. Treloar, *J. Gemmol.* **2013**, *33*, 161.
[16] B. M. Loeffler, R. G. Burns, *Am. Sci.* **1976**, *64*, 636.
[17] C. P. Smith, *Gems Gemol.* **2011**, *47*, 119.
[18] P. Thongnopkun, P. Chanwanitsakun, *IOP IOP Conference Series: J. Phys. Conf. Ser.* **2018**, *1144*, 012183.
[19] D. Lauwers, A. Candeias, A. Coccato, J. Mirao, L. Moens, P. Vandenabeele, *Spectrochim. Acta - Part a Mol. Biomol. Spectrosc.* **2016**, *157*, 146.
[20] S. Karampelas, L. Kiefert, D. Bersani, P. Vandenabeele, *Gems and Gemmology: An Introduction for Archaeologists, Art-historians and Conservators*, Springer Nature, Switzerland **2020**, pp. 1.
[21] G. Barone, D. Bersani, P. Mazzoleni, S. Raneri, *Open Archaeol.* **2017**, *3*, 194.
[22] G. Barone, D. Bersani, P. P. Lottici, P. Mazzoleni, S. Raneri, U. Longobardo, *J. Raman Spectrosc.* **2016**, *47*, 1534.
[23] G. Barone, P. Mazzoleni, S. Raneri, J. Jehlička, P. Vandenabeele, P. P. Lottici, G. Lamagna, A. M. Manenti, D. Bersani, *Appl. Spectrosc.* **2016**, *70*, 1420.
[24] G. Barone, D. Bersani, V. Crupi, F. Longo, U. Longobardo, P. P. Lottici, I. Aliatis, D. Majolino, P. Mazzoleni, S. Raneri, V. Venuti, *J. Raman Spectrosc.* **2014**, *45*, 1309.
[25] D. Bersani, G. Azzi, E. Lambruschi, G. Barone, P. Mazzoleni, S. Raneri, U. Longobardo, P. P. Lottici, *J. Raman Spectrosc.* **2014**, *45*, 1293.
[26] D. Bersani, P. P. Lottici, *Anal. Bioanal. Chem.* **2010**, *397*, 2631.
[27] P. Vandenabeele, M. K. Donais, *Appl. Spectrosc.* **2016**, *70*, 27.
[28] P. Vandenabeele, H. G. M. Edwards, J. Jehlička, *Chem. Soc. Rev.* **2014**, *43*, 2628.
[29] S. Eaton-magaña, C. M. Breeding, *Gems Gemmol.* **2016**, *52*, 2.
[30] G. R. Rossman, *Elements* **2009**, *5*, 159.
[31] D. Joseph, M. Lal, P. S. Shinde, B. D. Padalia, *X-Ray Spectrom.* **2000**, *29*, 147.
[32] L. Pappalardo, A. G. Karydas, N. Kotzamani, G. Pappalardo, F. P. Romano, C. Zarkadas, *Nucl. Instrum. Methods Phys. Res. B.* **2005**, *239*, 114.
[33] S. Eaton-magaña, C. M. Breeding, A. C. Palke, A. Homkrajae, Z. Sun, G. McElhenny, *Minerals* **2021**, *11*, 1.
[34] C. Lenz, L. Nasdala, D. Talla, C. Hauzenberger, R. Seitz, U. Kolitsch, *Chem. Geol.* **2015**, *415*, 1.
[35] F. A. Weis, P. Lazor, H. Skogby, R. Stalder, L. Eriksson, *Eur. J. Mineral.* **2016**, *28*, 537.
[36] C. M. MacRae, N. C. Wilson, *Microsc. Microanal.* **2008**, *14*, 184.
[37] R. Jasinevicius, Master's degree thesis, University of Arizona **2009**, 147.
[38] E. Fritsch, B. Rondeau, T. Hainschwang, S. Karampelas, in *Raman Spectroscopy Applied to Earth Sciences and Cultural Heritage*, (Eds: J. Dubessy, M.-C. Caumon, F. Rull), Mineralogical Society of Great Britain and Ireland, Twickenham, UK **2012**.
[39] B. Koziarska, M. Godlewski, A. Suchocki, M. Czaja, Z. Mazurak, *Phys. Rev. B* **1994**, *50*, 12297.
[40] G. Giuliani, D. Ohnenstetter, F. Palhol, J. Feneyrol, E. Boutroy, H. De Boissezon, T. Lhomme, *Can. Mineral.* **2008**, *46*, 1183.
[41] G. Giuliani, J. Dubessy, D. Ohnenstetter, D. Banks, Y. Branquet, J. Feneyrol, A. E. Fallick, J. E. Martelat, *Miner. Deposita* **2018**, *53*, 1.
[42] J. Saul, *Int. Geol. Rev.* **2018**, *60*, 889.
[43] S. Andò, E. Garzanti, *Geol. Soc. Spec. Pub.* **2014**, *386*, 395.
[44] Z. Mao, F. Jiang, T. S. Duffy, *Am. Mineral.* **2007**, *92*, 570.
[45] R. Wang, Y. Li, *Spectrosc. Lett.* **2011**, *44*, 432.
[46] M. Giarola, G. Mariotto, D. Ajò, *J. Raman Spectrosc.* **2012**, *43*, 556.
[47] D. Taylor, A. H. Rankin, P. J. Treloar, *J. Gemmol.* **2013**, *33*, 149.
[48] S. Harrison, J. A. Jaszczak, M. Keim, M. Rumsey, M. A. Wise, *Mineral. Rec.* **2014**, *45*, 553.

[49] V. A. Solé, E. Papillon, M. Cotte, P. Walter, J. Susini, *Spectrochim. Acta - Part B at. Spectrosc.* **2007**, *62*, 63.
[50] J. Jehlička, A. Culka, D. Bersani, P. Vandenabeele, *J. Raman Spectrosc.* **2017**, *48*, 1289.
[51] Bilbao Crystallographic Server, https://www.cryst.ehu.es/, (accessed 30 April 2021).
[52] W. Dollase, *Am. Mineral.* **1968**, *53*, 1882.
[53] Zoisite R050038 - RRUFF Database: Raman, X-ray, Infrared, and Chemistry, https://rruff.info/Zoisite/R050038, (accessed 9 April 2021).

SUPPORTING INFORMATION

Additional supporting information may be found online in the Supporting Information section at the end of this article.

How to cite this article: A. Coccato, D. Bersani, M. C. Caggiani, P. Mazzoleni, G. Barone, *J Raman Spectrosc* **2022**, *53*(3), 550. https://doi.org/10.1002/jrs.6203